INVESTIGATIONS ON CENTRIFUGAL PUMPS UNDER AIR ENTRAINMENT CONDITIONS

T. Schäfer[1,*], A. Bieberle[1] and U. Hampel[1,2]

[1]Helmholtz-Zentrum Dresden - Rossendorf, Institute of Fluid Dynamics,
Bautzner Landstraße 400, 01328 Dresden, Germany
[2]AREVA Endowed Chair of Imaging Techniques in Energy and Process Engineering,
Technische Universität Dresden, 01062 Dresden, Germany
thomas.schaefer@hzdr.de; a.biebrle@hzdr.de; u.hampel@hzdr.de

ABSTRACT

In this work, high-resolution gamma-ray computed tomography was applied to investigate the two-phase distribution in the impeller region of an industrial centrifugal pump. As an advanced tomographic method time-averaged rotation-synchronized computed tomography method has been successfully applied in addition to conventional radiography to investigate the internal gas-liquid two-phase flow. The formations of the gas holdups in different heights near to the shaft and in the impeller wheel, depending on the injected gas volume fraction, have been analyzed and the consequences on the pump operation have been discussed. Furthermore, internal accumulated gas holdup pattern and pump performance depending on the inlet gas volume fraction and inlet flow regimes have been investigated. Thus, influences of different flow regimes on the internal gas-holdup have been identified. Moreover, calculated gas holdup profiles in the six impeller chambers of the impeller wheel have been analyzed along selected streamlines. As a result, typical holdup profiles have been evaluated.

1. INTRODUCTION

1.1. Centrifugal pumps

Centrifugal pumps are widely used in process industries and power engineering, e.g. in refineries as feeding pumps or in power plants in cooling circuits. In nuclear power plants they are operated in various places and particularly in safety-related functions, like emergency core cooling. In chemical industries these flow machines are used to transport inorganic and organic liquids as well. Furthermore, other applications of centrifugal pumps can be found in water treatment, oil industries, food production and agriculture, heating installations or shipbuilding industries.

In general centrifugal pumps consist of an impeller and a diffusor. The rotating impeller is used to transfer the mechanical energy from the driving shaft into the fluid. This occurs by flow acceleration and flow redirection. Thus, the kinetic energy of the fluid increases. The diffusor is necessary to convert the imparted kinetic energy of the fluid into pressure energy. This leads to an increasing pressure, which drives the flow.

Though simple in design centrifugal pumps offer advantages, like high operational efficiency and low energy consumption, smooth and steady operation and high reliability. They produce a very steady,

consistent and even flow, which is requested for many applications. Further advantages are their higher discharging capacity, higher operating speeds and their ability for lifting highly viscous liquids such as oil and sewage water, sugar molasses or paper pulp. Due to these advantages they are the favorite choice in many applications.

However, centrifugal pumps also come with some deficiencies. Their major disadvantages are the tendency to vortex formation at suction side, vibrations and noise. Also the possibility of occurring of cavitation at higher flow rates is problematical. As reported by [1] the cavitation characteristics and performance of a pump is influenced by the blade number, which is one of the most important design parameters of centrifugal pumps.

1.2. Gas entrainment

Gas entrainment as well as internal steam generation by cavitation is known as being detrimental and critical to the operation of centrifugal pumps, since they were primarily designed for single phase operation. Gas entrainment decreases the efficiency of the pump and can result in negative influences on the plant performance. Unfortunately it is not always possible to avoid the entrainment of gas. For instance, gas entrainment may occur in situations, where water is conveyed from a reservoir with a shallow liquid height. There hollow vortices may form as a consequence of low liquid level and pre-existing fluid swirling. Particularly, such a situation may be prevailing in nuclear power plants, e.g. when emergency cooling water is taken from a liquid reservoir, like the condensation chamber. Thus the effects of gas entrainment on centrifugal pumps have to be analyzed and its effects on the flow regime as well as the influences on the pump characteristics have to be clarified, with respect to the general plant safety.

1.3. Previous work

Several studies have been made, investigating the behavior and characteristics of centrifugal pumps under general working conditions [2-4]. Thus, the adverse impacts of entrained gas on the characteristics of centrifugal pumps were observed. Presence of gas in pumps may lead to abrasion at impeller blades, strong vibrations with damaging of bearings and loss of cooling for shaft and bearings and early fatigue as a consequence. At least the presence of gas will lead to decreasing pump performance even to the point of abrupt collapse of flow rate.

Up to now, the effects of air entrainment have been investigated under various operating conditions [5-6], but the characteristics of gas phase fraction accumulation inside centrifugal pumps, particularly in the impeller and nearby the shaft seal region, are insufficiently understood. As reported by [7] the gas behavior depends on distributions of static pressure and liquid velocity in the impeller passages. Already, the changes in pressure, velocities and void fraction distribution under two phase flow conditions were calculated, solving the Reynolds-averaged Navier-Stokes equations for two phase flow in the impeller region of a centrifugal pump [8]. Flow-induced pressure pulsations, vibrations and the resulting noise were investigated in a centrifugal pump [2]. Several experiments on cavitating flows in a centrifugal pump with two dimensional curved blades were conducted in the past, to find out the cavitation characteristics and to develop a numerical model to predict the cavitation behavior [9]. Recently, the flow conditions during fast start up which can cause cavitation were investigated in a centrifugal pump with open impeller [10] and in a modified centrifugal pump using x-ray measurements [11]. For different flow conditions simulations of cavitating flow in a centrifugal pump were conducted [12]. Here the investigations were focused on low flow rates. Related to this, the unsteady flow structure which appears for example in pressure fluctuations were investigated under single phase conditions for a low specific speed centrifugal pump using a numerical model [3]. Moreover, studies on different impellers were carried out, to optimize the hydrodynamic performance of a centrifugal pump by an improved impeller design [13-14].

However, the investigations on centrifugal pumps, which are designed for single phase flow, but working under two phase flow conditions, have to be continued, since the behavior of the appearing flow and its effects on the characteristics of the centrifugal pumps are insufficient understood. Experimental investigations on pump characteristics and performance breakdown at different flow conditions under air entrainment conditions are essential to increase the efficiency of centrifugal pumps. Based on these analyses, advisable working conditions can be defined and the geometric design can be improved. Also further investigations and experiments which deliver temporal and spatial high-resolution data sets are required. They may help to identify characteristic flow structures in more detail. The results of these investigations are beneficial in the field of scientific research to get a better understanding of the physics of the multiphase flow which is helpful for example to find better flow models for computational fluid modelling. But they are also significant in industries for plant operators and pump manufactures since it can be used to avoid operational problems, increasing the plant energy efficiency or for the development and engineering of optimized pumps.

2. MATERIALS AND METHODS

2.1. Experimental Setup

For investigations on centrifugal pumps, a hydraulic test facility was designed and built up. Thus, two-phase flows with defined adjustable gas volume fractions can be provided at the suction side of the centrifugal pump. Additionally, two specific gas phase fraction arrangements are selectable.

In general, the hydraulic test facility consists of two main components, which are a supply part and a modular test section. A two staged separator which is used as liquid feeding reservoir as well as for the separation of the recirculated two phase flow is integrated in the supply part. Furthermore, a heat exchanger (C200 301-1, FUNKE, Germany) is implemented. The test facility is instrumented with a magnetic inductive liquid flow meter (MAG 1100, Siemens, Germany) and a temperature sensor (PT100) to measure the liquid temperature T_L. The temperature is controlled by a thermostat (Unistat Tango) in combination with the heat exchanger. Thus, isothermal conditions are guaranteed during the experiments. Furthermore, the pressure at the suction side of the centrifugal pump p_{suc} as well as the differential pressure across the pump Δp_{pump} is measured.
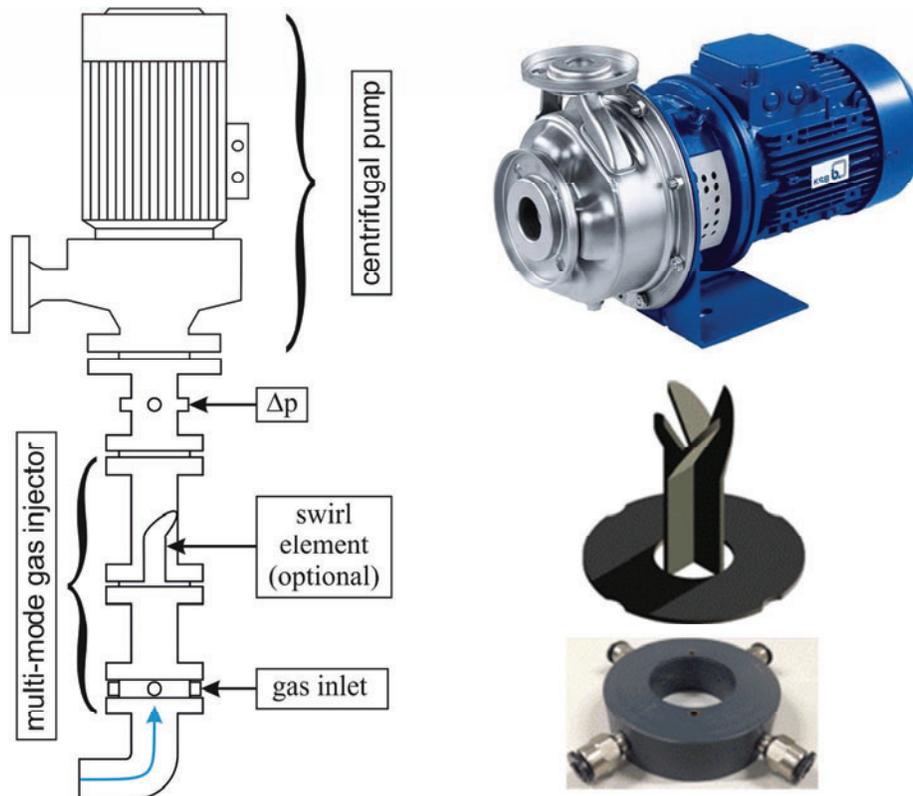
Figure 1. Simplified scheme of the modular pump test section with multi-mode gas injection module and investigated centrifugal pump.

The centrifugal pump, which is under investigation (Etachrom BC 032-160/074 C11, KSB, Germany), is installed in a way, that its impeller wheel is horizontally aligned. The centrifugal pump has a DN 50 inlet and a DN 32 outlet. It drives the flow loop of the experimental rig and is part of the modular pump test section (Figure 1).

Additionally, another essential component is the multi-mode gas injection module which is also illustrated in Figure 1. It consist of a gas injection ring with four hole type nozzles, for the disperse injection of gas (purified compressed air). The nozzles are arranged symmetrically around the pipe. The gas injection ring can be combined with a special designed swirl element. Thus, a dispersed gas-liquid two-phase flow as well as a two-phase vortex flow with formed gas core can be generated at the suction side of the centrifugal pump. The injected gas flow rate Q_G is controlled by a mass flow controller (FMA-2600, OMEGA Newport). It is calculated according to

$$Q_G = \frac{\varepsilon_{in}}{1-\varepsilon_{in}}\, Q_L \quad for\ 0 \leq \varepsilon_{in} < 1\ and\ Q_L \neq 0, \tag{1}$$

using the current liquid flow rate Q_L and a given inlet gas volume fraction ε_{in}. The facility can be completely controlled with a programmable logic control (SPS-ILC 350 ETH, Phoenix Contact) via a web interface. The experimental conditions data, like flow rates, pressures and temperatures, are stored in a data base synchronized to the tomographic scan data sets by time stamps.

2.2. High-Resolution Gamma-Ray Computed Tomography Scanner

High-resolution gamma-ray computed tomography (HIRE-CT) has been chosen to determine the gas phase distribution in an industrial centrifugal pump quantitatively, since it was already successfully

applied on hydrodynamic test facilities, e.g. in bubble columns [15-16], axial pumps [17], fluid couplings [18-19], trickle bed reactors [20] and electrically heated rod bundles [21].

The HIRE-CT scanner is able to scan objects with a typical spatial resolution of about 2 mm and with a maximal object diameter of up to 700 mm. A multi-pixel detector arc, consisting of 320 scintillation detectors (8e-6 sqm active area) is arranged in a horizontal plane, surrounding the scanned object. It is aligned with an isotopic source (^{137}Cs, energy = 662 keV, activity = 180 GBq) to measure transmitted gamma radiation and, thus, provides projection raw data sets for subsequent image reconstruction.

Especially the usage of isotopic sources, emitting high mono-energetic gamma photons, allows analyses within industrial-authentically operated facilities since wall thicknesses of many centimeters of steel can be easily penetrated. As a result, 2-D or 3-D material distributions can be obtained contactless and without interfering with the internal processes. Further details of the used HIRE-CT scanner can be found in [22].

2.3. Scanning Modes and Data Processing

Conventional radiography scanning mode [23] and time-averaging rotation-synchronized computed tomography scanning mode [17] have been applied. For the conventional radiography scanning mode, the centrifugal pump is positioned in the HIRE-CT scanner between the isotopic source and the detector arc. The isotopic source emits gamma radiation which is differently attenuated by the scanned object (centrifugal pump), depending on its structure and materials. The penetrated radiation represents the material distribution of the object along various ray paths as a projection of the attenuation properties. It is detected by scintillation detectors of the detector arc, for an adequate time, and subsequently recorded. Afterwards, this procedure is repeated for several heights, which means closely spaced, intersecting scanning planes through the object (vertical spacing: inside the impeller wheel 2 mm, else 3 mm). Eventually, all recorded projections from different scanning planes are appended and thus, a two-dimensional radiographic image (attenuation image) of the scanned object is obtained.

To obtain cross-sectional tomographic images time-averaging rotation-synchronized computed tomography scanning mode has been used. Differing from conventional computed tomography scanning mode, there is no mechanical rotating source-detector unit required. Instead, the inherent rotation of the pump impeller wheel is directly used to generate the necessary set of projections of the scanned object (Figure 2). Therefore, the projection data acquisition is synchronized to the impeller rotation positon. This can be realized with a HALL sensor, which is installed closely to the driving shaft of the centrifugal pump.

While the conventional radiography delivers integral gas phase fraction distributions according to the scanning planes in different heights, the time-averaging rotation-synchronized computed tomography scanning mode discloses the spatial distribution of the gas phase fraction, which is accumulated in the rotating impeller wheel of the centrifugal pump.
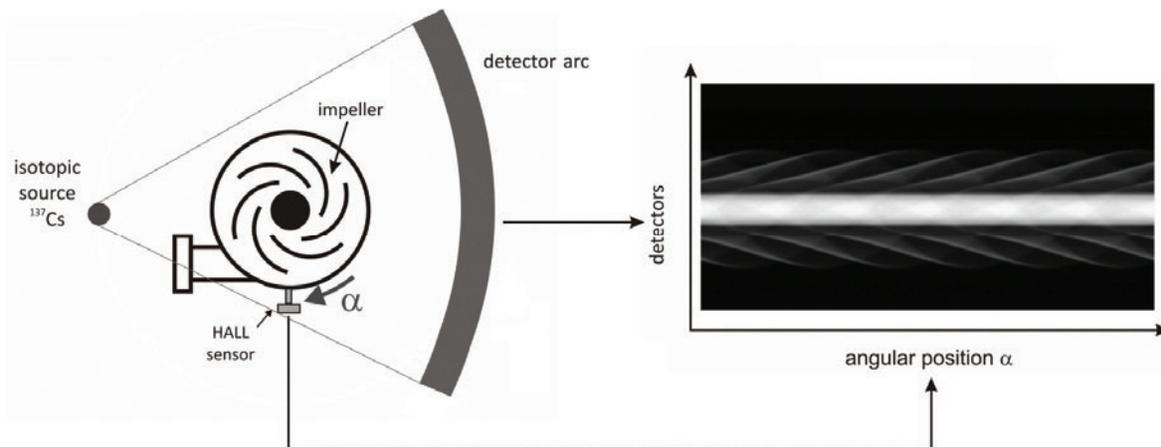
Figure 2. Principle of time-averaging rotation-synchronized computed tomography scanning mode.

For tomographic image reconstructions algebraic reconstruction technique (ART) according to [24] is used

$$\mu_{i,j}^{(\tau+1)} = \mu_{i,j}^{(\tau)} + \lambda \frac{a_{i,j,d,p}\left(E_{d,p} - \sum_{i=1}^{N_x}\sum_{j=1}^{N_y} a_{i,j,d,p}\mu_{i,j}^{(\tau)}\right)}{\sum_{i=1}^{N_x}\sum_{j=1}^{N_y} a_{i,j,d,p}^2}. \tag{2}$$

Here, $\mu_{i,j}$ are the cross-sectional attenuation coefficients, $E_{d,p}$ are the total attenuation data, i and j represent indices of the image pixels, N_x and N_y represent the dimensions of the reconstructed attenuation image, λ is the relaxation factor, τ is the current number of iteration steps, and $a_{i,j,d,p}$ are weights, which are given by the spatial overlap of a pixel (i,j) with a ray (d,p). In this work, reconstruction was performed on a sufficiently large regular pixel grid of $N_x = N_y = 320$ and with 1 mm × 1 mm pixel size.

A phase fraction distribution can then be quantitatively determined by scaling the reconstructed cross-sectional attenuation coefficient distributions on reference CT scans from the object operated with each phase (liquid, gas) separately.

The spatial resolution in the phase fraction distribution based on the reconstructed tomographic images is about 1 mm but depends slightly on the radial position inside the scanning plane and is also affected by the geometric structure and material distribution of the object. Further limitations of the image quality arise from reconstruction artefacts, image noise and random noise in the electronic measurement signals as well as scattered radiation. The appearance of reconstruction artefacts also depends on the particular object and its structure. Applying suitable additional processing steps for example scatter correction can reduce such effects effectively.

3. RESULTS

3.1. Gas Holdups in the Centrifugal Pump in Different Heights

In a first step, the formations of the gas holdups in different heights near to the shaft and in the impeller wheel, depending on the injected gas volume fraction, were analyzed. Therefore, radiographic scans were performed under different two phase flow operating conditions. Additionally, the centrifugal pump was completely filled with water and a reference scan was recorded. Based on this scans, the vertical distribution of the gas holdup in the centrifugal pump were calculated. Eventually, the obtained results

were overlaid on a radiography of the non-operating and drained centrifugal pump, which serves for the representation of the housing and the internal structure of the investigated centrifugal pump in the radiographic images (Figure 3).
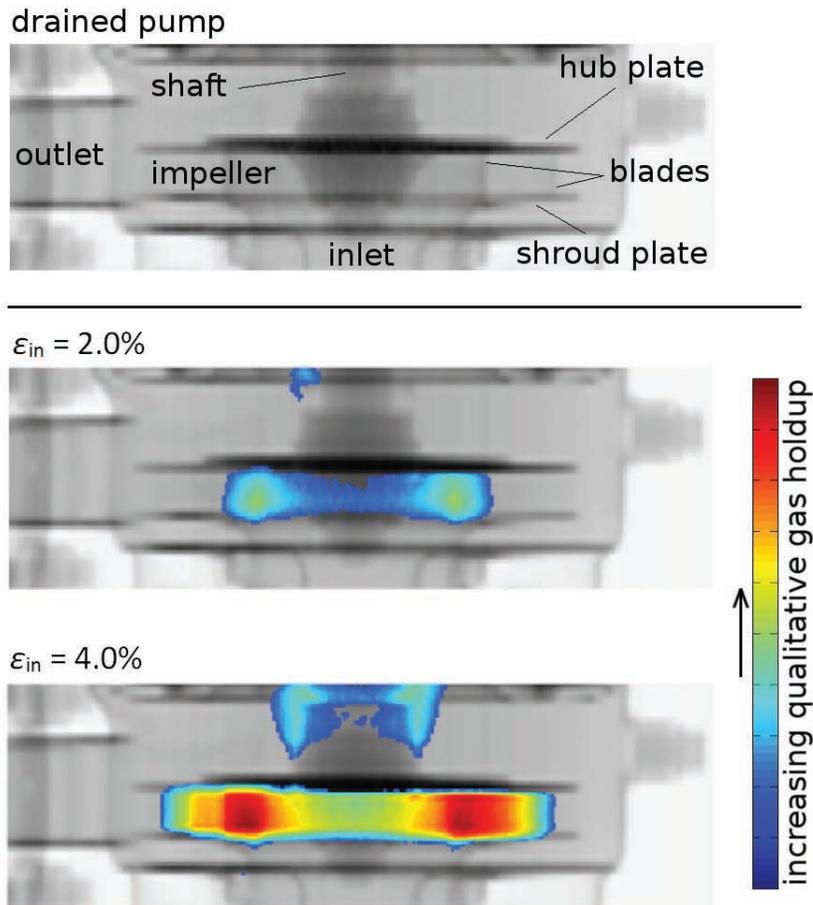
Figure 3. Radiographies of typical vertical gas holdup formations near to the shaft and inside the impeller wheel, depending on two different inlet gas volume fractions. For better illustration all regions fully liquid are not represented in the radiographies.

The formation of typical vertical gas holdup distributions near to the shaft, depending on the inlet gas volume fraction is observable. Furthermore, the independence of vertical holdup formation inside the impeller can be identified. The obtained results show very clearly, that the lubrication and cooling of the shaft seal is warranted only for very small inlet gas volume fractions in the suction side flow under air entraining flow conditions. Thus, a perpetual application under these operating conditions may lead to an early fatigue of the shaft bearings.

3.2. Centrifugal Pump Performance Dependence on Inlet Flow Regimes

Furthermore, the internal accumulated gas holdup pattern and pump performance depending on the inlet gas volume fraction and inlet flow regimes were investigated (diagram in Figure 4). It can be determined, that the pump performance decreases with increasing inlet gas volume fraction, which is less remarkable since it can be expected. This happens due to the reduced momentum transfer from the impeller to the

fluid because of the present gas. But, furthermore, an untypical discontinuity in the pump performance is detectable, depending on the inlet flow regime.

While the conveying curve decreases nearly linearly under intake conditions with disperse entrained gas, there is a significant discontinuity in the conveying curve for entrained gas volume fractions between ε_{in} =2.5% and ε_{in} = 3.0% which are entrained with a swirling flow. Under these conditions there is an abrupt and reproducible decrease of the pump performance. Furthermore, also nearly similar holdup pattern are observable for the different intake flow regimes at completely different inlet gas volume fraction of ε_{in} = 3% and ε_{in} = 5%.

Based on these results, optimal inlet flow regimes, in terms of the centrifugal pump performance under air entraining conditions, can be evaluated. It becomes apparent, that disperse entrained gas is preferable against gas which is entrained with a swirling flow. This means in practice, that, if there is an unavoidable gas entrainment, the pump operator has to carry for suitable intake conditions (disperse entrained gas) using appropriate technical interventions, such as static mixers, for example.
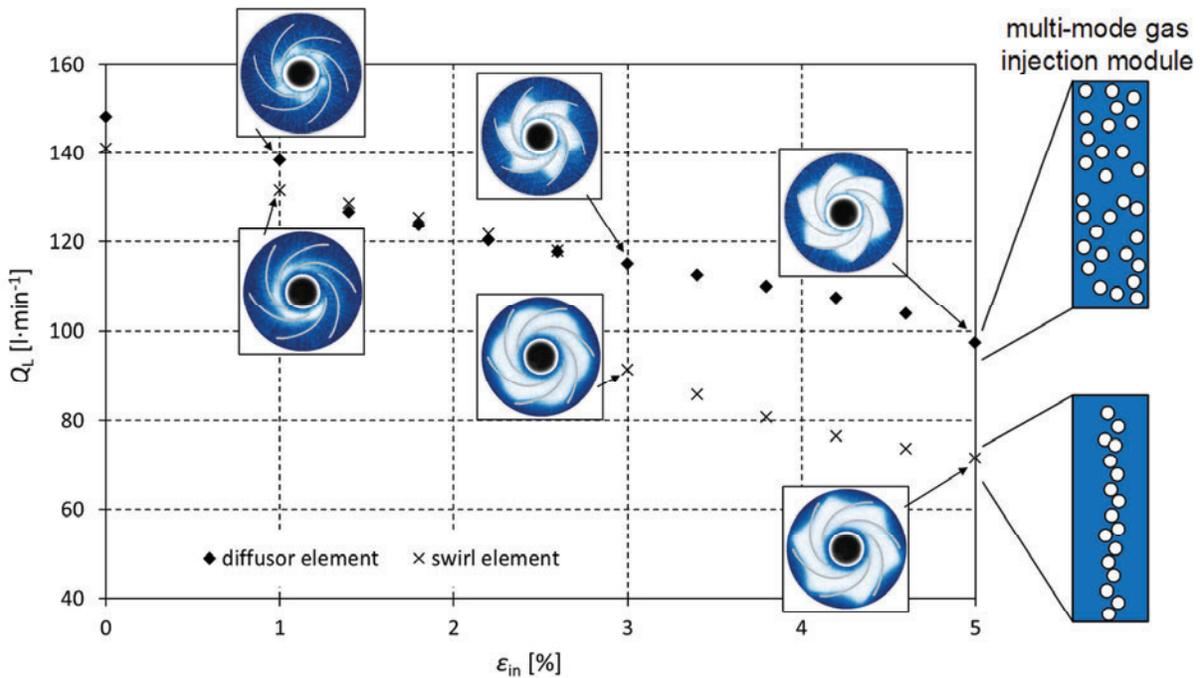
Figure 4. Internal accumulated gas holdup pattern and pump performance depending on the inlet gas volume fraction and inlet flow regimes.

3.3. Gas Holdup Profiles along Selected Streamlines

The gas holdup profiles in the six impeller chambers were analyzed along selected streamlines. These selected streamlines are illustrated as colored lines in Figure 5. For the calculations of the gas holdup profiles along these selected streamlines, the phase fraction distributions based on the reconstructed tomographic images were interpolated (bicubic, up to 1560x1560px). This means the actual spatial resolution of the measured phase fraction distributions based on the reconstructed tomographic images remains unaffected (1 mm), since it is given by the measurement system, but the grid for the subsequent calculations of the holdup profiles along the streamlines is finer.

The obtained gas holdup profiles along these selected streamlines for the six impeller chambers are represented in the diagrams in Table I for ε_{in} = 3% and for an impeller revolution of 1900 rpm.

The analysis of these holdup profiles discloses several remarkable details. For the impeller chambers 1 to 5, it is clearly visible, that in the inner area of the impeller (radii between 27 mm and 47 mm) the gas holdup along the center and suction side streamlines is slightly higher than along the pressure-side streamline. But for the impeller chamber 6 the holdup profiles are completely different. Here, the gas holdup along the pressure-side streamline is nearly similar, compared to the chambers 1 to 5, while the gas holdup along the center and suction side streamlines is much smaller than along the pressure-side streamline. An explanation for this observed noticeable gas holdup behavior has been given by another investigation [25], which indicated clearly, that the deviant distribution is caused by a balancing hole, which is placed in the hub side plate of the 6th impeller chamber.

Furthermore, for all selected streamlines and in all impeller chambers a concordant gas holdup value can be discovered at a radius of about 47 mm. At this radial position a transition of the gas holdup distribution from the inner impeller area to the outer one takes place. This means, a large part of the accumulated gas in the impeller chamber relocates from the suction-side streamline to the pressure-side streamline.
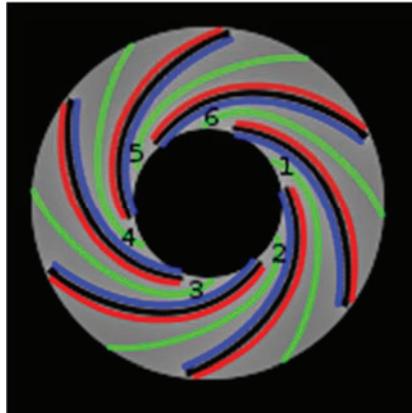
Figure 5. Illustration of pressure-side streamlines (red), center streamlines (green) and suction-side streamlines (blue), which were selected for the analysis of the gas holdup profiles in the six impeller chambers.

Table I. Gas holdup profiles along selected streamlines for the six impeller chambers for $\varepsilon_{in} = 3\%$ and for an impeller revolution of 1900 rpm.
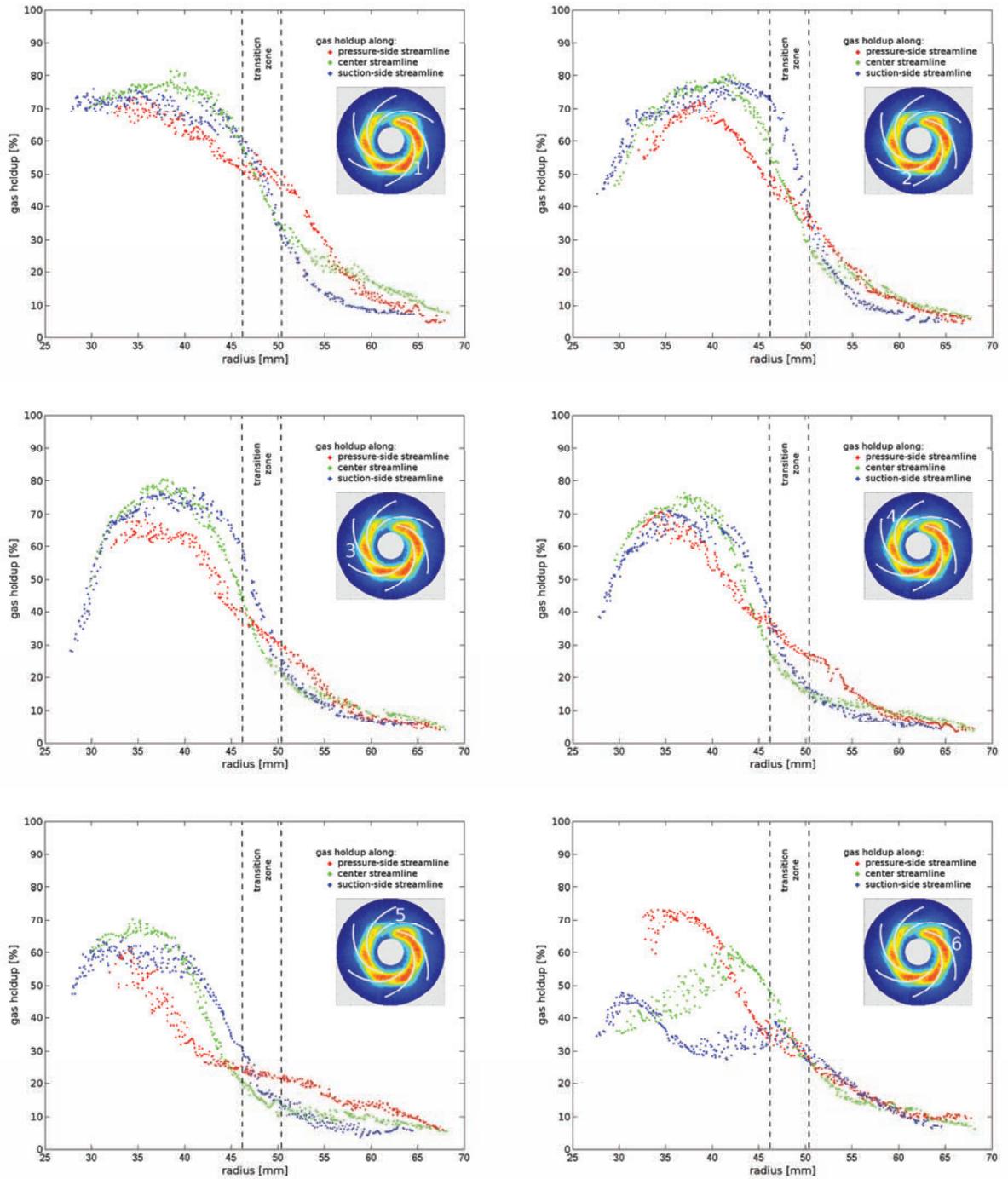
4. CONCLUSIONS

The presented work contributes quantitative measurements, visualizations and analyses of gas-liquid phase distributions to the fundamental understanding of the effects of gas entrainment in centrifugal pumps. High-resolution gamma-ray computed tomography was applied to investigate the two-phase distribution in the impeller region of an industrial centrifugal pump. Time-averaged rotation-synchronized computed tomography method and conventional radiography has been successfully applied to investigate the gas-liquid two-phase distribution in an industrial centrifugal pump. Applying these computed tomography techniques, the local distribution of the gas-holdup inside the rotating impeller were captured with very high spatial resolution. Thus, the influences of different flow regimes on the internal gas-holdup have been identified. The obtained data are a basis for the modeling of the gas accumulation in centrifugal pumps under air entraining conditions and the effects occurring thereby. Based on this, CFD simulations can be validated and design modifications and optimizations of the centrifugal pumps can be derived.

ACKNOWLEDGMENTS

REFERENCES

1. H. Liu, J. Wang, S. Yuan, M. Tan, K. Wang, "Effects of Blade Number on Characteristics of Centrifugal Pumps," *Chinese Journal of Mechanical Engineering*, **23**, pp. 1-6, (2010).
2. A. Suhane, "Experimental study on centrifugal pump to determine the effect of radial clearance on pressure pulsations vibrations and noise," *International Journal of Engineering Research and Applications* **2**(4), pp. 1823-1829, (2012).
3. J. Gonzalez, C. Santolaria, "Unsteady flow structure and global variables in a centrifugal pump," *Journal of Fluids Engineering* **128,** pp. 937-946, (2006).
4. L. Zhou, W. Shi, S. Wu, "Performance optimization in a centrifugal pump impeller by orthogonal experiment and numerical simulation," *Advances in Mechanical Engineering* **2013**(385809), pp. 1-7, (2013).
5. G. Caruso, L. Cristofano, M. Nobili, D. Vitale Di Maio, "Experimental investigation of free surface vortices and definition of gas entrainment occurrence maps," *Journal of Physics* **501**(012019) pp. 1-10, (2014).
6. N. Kimura, T. Ezure, A. Tobita, H. Kamide, "Experimental study on gas entrainment at free surface in reactor vessel of a compact sodium-cooled fast reactor," *Journal of Nuclear Science and Technology* **45**(10) pp. 1053-1062, (2008).
7. S. Sato, A. Furukawa, Y. Takamatsu, "Air-WaterTwo-Phase Flow Performance of Centrifugal Pump Impellers with Various Blade Angles," JSME International Journal Series B **39**(2), pp.223-229, (1996).
8. E.T. Pak, J.C. Lee, "Performance and pressure distribution changes in a centrifugal pump under two-phase flow," *Proc. Inst. Mech. Eng.* **212** pp. 165-171, (1998).
9. O. Coutier-Delgosha, R. Fortes-Patella, J.L. Rebound, "Hofmann, M.; Stoffel, B. Experimental and numerical studies in a centrifugal pump with two-dimensional curved blades in cavitating condition," *Journal of Fluids Engineering* **125** pp. 970-977, (2003).
10. Y. Zhang, Z. Zuchao, Y. Jin, B. Cui, Y. Li, H. Dou, "Experimental study on a centrifugal pump with open impeller during start-up period," *Journal of Thermal Science* **22**(1) pp. 1-6, (2013).
11. S. Duplaa, O. Coutier-Delgosha, A. Dazin, G. Bois, "X-Ray measurements in a cavitating centrifugal pump during fast start-ups," *Journal of Fluids Engineering* **135** pp. 041204/1-041204/9, (2013).
12. L. Tan, B.S. Zhu, S.L. Cao, Y.M. Wang, "Cavitation flow simulation for a centrifugal pump at low flow rate," *Chinese Science Bulletin* **58**(8) pp. 949-952, (2013).

13. A.V. Grapsas, J.S. Anagnostopoulos, D.E. Papantonis, "Experimental and numerical study of a radial flow pump impeller with 2D-curved blades," *Proceedings of the 5th IASME/WSEAS International Conference on Fluid Mechanics and Aerodynamics*, Athens, Greece, August 25-27 (2007).

14. L. Zhou, W. Shi, S. Wu, "Performance optimization in a centrifugal pump impeller by orthogonal experiment and numerical simulation," *Advances in Mechanical Engineering* **2013**(385809) pp. 1-7, (2013).

15. A. Kemoun, B.C. Ong, P. Gupta, M. Al-Dahhan, M.P. Dudukovic, "Gas holdup in bubble columns at elevated pressure via computed tomography," *International Journal of Multiphase Flow* **27** pp. 929-946, (2007).

16. U.P. Veera, "Gamma ray tomography design for the measurement of hold-up profiles in two-phase bubble columns," *Chemical Engineering Journal* **81** pp. 251-260, (2001).

17. H.-M. Prasser, D. Baldauf, J. Fietz, U. Hampel, C. Zippe, J. Zschau, M. Christen, G. Will, "Time resolving gamma-tomography for periodically changing gas fraction fields and its application to an axial pump," *Flow Measurement and Instrumentation* **14** pp. 119-125, (2003).

18. U. Hampel, D. Hoppe, K.-H.Diele, J. Fietz, H. Hoeller, R. Kernchen, H.-M. Prasser, C. Zippe, "Application of gamma tomography to the measurement of fluid distributions in a hydrodynamic coupling," *Flow Measurement and Instrumentation* **16** pp. 85-90, (2005).

19. U. Hampel, D. Hoppe, A. Bieberle, R. Kernchen, K.-H. Diele, E. Schleicher, M. J. Da Silva, C. Zippe, "Measurement of fluid distributions in a rotating fluid coupling using high resolution gamma ray tomography," *Journal of Fluids Engineering - Transactions on ASME* **130**(9) p. 091402, (2008).

20. M. Schubert, G. Hessel, C. Zippe, R. Lange, U. Hampel, "Liquid flow texture analysis in trickle bed reactors using high-resolution gamma ray tomography," *Chemical Engineering Journal* **140**(1-3) pp. 332-340, (2008).

21. A. Bieberle, D. Hoppe, E. Schleicher, U. Hampel, "Void measurement using high-resolution gamma-ray computed tomography," *Nuclear Engineering and Design* **241**(6) pp. 2086-2092, (2009).

22. U. Hampel, A. Bieberle, D. Hoppe, J. Kronenberg, E. Schleicher, T. Suehnel, W. Zimmermann, C. Zippe, "High resolution gamma ray tomography scanner for flow measurement and non-destructive testing applications," *Review of Scientific Instruments* **78**(10) p. 103704, (2007).

23. A.C. Kak, M. Slaney, *Principles of Computerized Tomography*, IEEE Press, New York, (1987).

24. R. Gordon, R. Bender, G.T. Herman, "Algebraic Reconstruction Techniques (ART) for three-dimensional Electron Microscopy and X-ray Photography," *J. Theor. Biol.* **29** pp. 471-481, (1970).

25. T.Schäfer, A.Bieberle, M. Neumann, U. Hampel, "Application of gamma-ray computed tomography for the analysis of gas holdup distributions in centrifugal pumps," *Flow Measurement and Instrumentation*, (forthcoming 2015), doi: 10.1016/j.flowmeasinst.2015.06.001.